ELSEVIER

Journal of Materials Processing Technology 79 (1998) 79–85

Journal of Materials Processing Technology

An improved model for oblique cutting and its application to chip-control research

N. Fang *

Department of Mechanical Engineering, Nanjing University of Aeronautics and Astronautics, Jiangsu 210016, People's Republic of China

Received 22 January 1997

Abstract

The traditional model for oblique cutting has two shortcomings, one being that it involves only one machining case where the tool major cutting edge angle is limited to be 90°, i.e. the undeformed chip thickness is equal to the feed of the tool; whilst the other is that it takes no account of the influence of the tool feed velocity on the resultant cutting velocity. In this present work, an improved model for oblique cutting is developed in which the influences of the two above factors, i.e. the tool major cutting edge angle and the tool feed velocity, on machining processes are considered. The new cutting model can be used to determine precisely some important parameters involved in machining processes, e.g. the effective rake angle of the tool, the effective shear angle and the consumption of cutting power, etc. As a practical example, the model that is established, combined with a theory on the minimum energy consumption, is used to carry out chip-control research. The chip flow direction and the chip flow speed are determined. The theoretically-predicted data is found to agree reasonably well with the experimental results under the given experimental conditions.

Keywords: Oblique cutting; Tool major cutting edge angle; Tool feed velocity; Chip control

1. Introduction

On the basis of the angular relationship between the cutting velocity vector and the cutting edge of the tool, different machining process can be classified into two categories, namely: (i) the orthogonal cutting process; and (ii) the oblique cutting process [1]. Great attention has been paid to oblique cutting by a number of researchers all around the world, because many practical machining processes are actually examples of oblique cutting, and numerous research papers have been published [2–7]. For reference books dealing with metal cutting [8–13] may be consulted.

However, it should be noted that most of the research is based on the traditional model for oblique cutting, shown in Fig. 1. The author of this paper thinks that there are two shortcomings in this model, as follows:

(1) It involves only one machining case where the tool major cutting edge angle is limited to be 90°, i.e. the undeformed chip thickness is equal to the feed of the tool. In the coordinate system shown in Fig. 1, o is any point at the tool major cutting edge, the z-axis is in the direction of the cutting velocity vector, the x-axis is parallel to the tool major cutting edge and the y-axis is perpendicular to the z- and x-axes. Due to the tool major cutting edge angle being 90°, the three measured force components of the resultant cutting force are along the x, y- and z-axes, respectively. The problem is that there exist many other practical machining cases where the tool major cutting edge angle is not always equal to 90°. Hence, some important parameters calculated from the traditional model, e.g. the effective rake angle of the cutting tool, the effective shear angle and the consumption of cutting power etc., can still not be used in the analysis of those machining processes.

(2) It takes no account of the influence of the tool feed velocity on the resultant cutting velocity. As a matter of fact, new research [14–17] has shown that this kind of influence cannot be neglected, especially in

* Present address: 700 Woodland Avenue C102, Lexington, KY 40508-3418, USA. Tel.: +1 606 2576262; e-mail: nfang@engr.uky.edu

0924-0136/98/$19.00
PII S0924-0136(97)00385-3

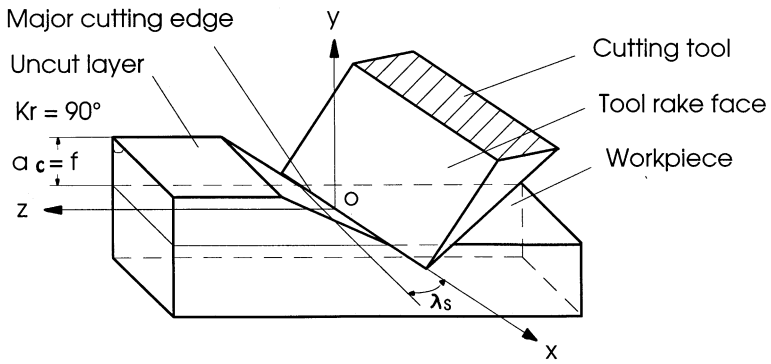

Fig. 1. Traditional model for oblique cutting (without showing the chip).

chip-control research. As is known, the tool feed velocity plays an important role in the resultant cutting velocity and has a great effect on chip flow and chip curl [18,19].

Therefore, in this present work, an improved model for oblique cutting is developed in which the influences of the two above factors, i.e. the tool major cutting edge angle and the tool feed velocity, on machining processes are considered. The new cutting model can be used to determine precisely some important parameters involved in machining processes, e.g. the effective rake angle of the tool, the effective shear angle and the consumption of cutting power, etc. As a practical example, the model, combined with a theory on the minimum energy consumption, is used to carry out chip-control research. The chip flow direction and the chip flow speed are determined from the model. The theoretically predicted data agrees reasonably well with the experimental results under the given experimental conditions.

2. Improved model for oblique cutting

Fig. 2 shows the improved model for oblique cutting, the chip not being shown to make the relating vectors clear.

In Fig. 2, o is any point at the tool major cutting edge. The z-axis is in the direction of the cutting velocity vector $\boldsymbol{V}_c$ (in this paper, in order to distinguish vectors from scalars, the bold-faced letters, $\boldsymbol{V}_c$, $\boldsymbol{V}_{ch}$, are used to denote vectors and the light-faced letters, V_c, V_{ch}, are used to denote scalars). The y-axis is in the opposite direction to the tool feed velocity vector $\boldsymbol{V}_f$, whilst the x-axis is perpendicular to the y- and z-axes. Line ol is the projection of the total major cutting edge on the xoy plane. The spatial position of the tool major cutting edge can be determined by the tool major cutting edge angle Kr and the tool cutting edge inclination angle λ_s. The spatial position of the tool rake face P_r can be determined by the tool major cutting edge and the normal rake angle of the tool γ_n. The chip flow direction makes an angle of η with the normal line of the tool major cutting edge on the tool rake face.

A series of important terms are defined as follows: (i) the resultant cutting velocity vector $\boldsymbol{V}$, the addition of the cutting velocity vector $\boldsymbol{V}_c$, and the tool feed velocity vector $\boldsymbol{V}_f$; (ii) the chip deformation plane P_d, the plane containing the resultant cutting velocity vector $\boldsymbol{V}$, and the chip flow velocity vector $\boldsymbol{V}_{ch}$, measured in P_d, the progressive deformation of an element of work material into the corresponding chip element being assumed to occur; (iii) the effective rake angle of the tool γ_e, the angle between the chip flow velocity vector $\boldsymbol{V}_{ch}$, and the tool base plane P_b (i.e. the xoy plane), measured in P_d; and (iv) the effective shear angle ϕ_e, the angle between the resultant cutting velocity vector $\boldsymbol{V}$, and the shear plane P_s, measured in P_d.

It is noteworthy that the above definitions of P_d, γ_e and ϕ_e are different from their respective traditional definitions in the literature [8].

3. Theoretical calculations based on the improved model

3.1. Two basic unit vectors

Supposing that $\boldsymbol{i}$, $\boldsymbol{j}$, $\boldsymbol{k}$ are, respectively, three unit vectors along the x-, y-, and z-axes, the unit vector in the tool rake face parallel to the tool major cutting edge $\boldsymbol{b}_0$ can be determined as:

$$\boldsymbol{b}_0 = \cos\lambda_s \sin Kr \cdot \boldsymbol{i} - \cos\lambda_s \cos Kr \cdot \boldsymbol{j} - \sin\lambda_s \cdot \boldsymbol{k} \quad (1)$$

The unit vector in the tool rake face perpendicular to the tool major cutting edge $\boldsymbol{a}_0$ can be found from:

$$\boldsymbol{a}_0 = a_{0x} \cdot \boldsymbol{i} + a_{0y} \cdot \boldsymbol{j} + a_{0z} \cdot \boldsymbol{k} \quad (2)$$

where:

$$a_{0x} = \cos\gamma_n \cos Kr - \sin\lambda_s \sin Kr \sin\gamma_n \quad (3a)$$

$$a_{0y} = \cos\gamma_n \cos Kr - \sin\lambda_s \sin Kr \sin\gamma_n \quad (3b)$$

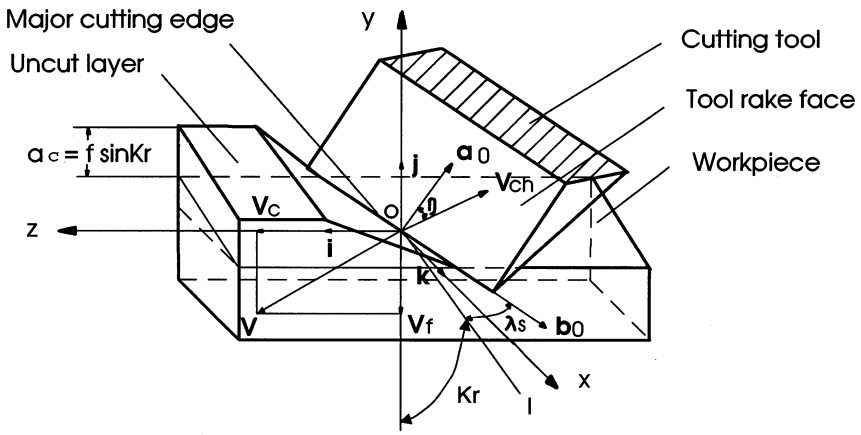

Fig. 2. Improved model for oblique cutting.

$$a_{0z} = -\sin\gamma_n \cos\lambda_s \tag{3c}$$

3.2. Some important velocity vectors

The unit vector parallel to the chip flow velocity vector $\boldsymbol{V}_{ch0}$ is:

$$\boldsymbol{V}_{ch0} = \boldsymbol{a}_0 \cdot \cos\eta + \boldsymbol{b}_0 \cdot \sin\eta = V_{ch0x} \cdot \boldsymbol{i} + V_{ch0y} \cdot \boldsymbol{j} + V_{ch0z} \cdot \boldsymbol{k} \tag{4}$$

$$V_{ch0x} = \cos\eta \cdot a_{0x} + \sin\eta \cdot \cos\lambda_s \cdot \sin Kr \tag{5a}$$

$$V_{ch0y} = \cos\eta \cdot a_{0y} - \sin\eta \cdot \cos\lambda_s \cdot \cos Kr \tag{5b}$$

$$V_{ch0z} = \cos\eta \cdot a_{0z} - \sin\eta \cdot \sin Kr \tag{5c}$$

The following equations hold:

$$\boldsymbol{V}_{ch} = V_{ch} \cdot \boldsymbol{V}_{ch0} \tag{6}$$

$$\boldsymbol{V}_c = -(\pi n D/1000) \cdot \boldsymbol{k} \tag{7}$$

$$\boldsymbol{V}_f = -(fn/1000) \cdot \boldsymbol{j} \tag{8}$$

$$\boldsymbol{V} = \boldsymbol{V}_c + \boldsymbol{V}_f \tag{9}$$

$$\boldsymbol{V}_0 = \boldsymbol{V}/V \tag{10}$$

where $\boldsymbol{V}_0$ is the unit vector parallel to $\boldsymbol{V}$, f is the feed of the tool per revolution, n is the speed of the spindle of machine tool and D is the diameter of the workpiece.

In accordance with the principles of kinematics, three velocity vectors, $\boldsymbol{V}$, $\boldsymbol{V}_{ch}$ and the shear velocity vector $\boldsymbol{V}_s$, involved in oblique cutting must form a closed velocity triangle, shown in Fig. 3. Thus, it is easy to obtain the following relationships:

$$\boldsymbol{V}_s = \boldsymbol{V}_{ch} - \boldsymbol{V} \tag{11}$$

$$\boldsymbol{V}_{s0} = \boldsymbol{V}_s/V_s \tag{12}$$

$$V_{ch} = V \cdot \sin\phi_e/\cos(\gamma_e + \phi''_e) \tag{13}$$

$$V_s = V \cdot \cos(\gamma_e + \phi''_e)/\cos(\gamma_e + \phi'_e) \tag{14}$$

where $\boldsymbol{V}_{s0}$ represents the unit vector parallel to $\boldsymbol{V}_s$.

3.3. Unit normal vectors of some planes and the plane equations

$$\boldsymbol{P}_{b0} = \boldsymbol{k} \tag{15}$$

$$\boldsymbol{P}_{d0} = P_{dox} \cdot \boldsymbol{i} + P_{doy} \cdot \boldsymbol{j} + P_{doz} \cdot \boldsymbol{k} \tag{16}$$

$$P_{dox} = \frac{\pi \cdot D \cdot V_{ch0y} - f \cdot V_{ch0z}}{\sqrt{f^2 + \pi \cdot D^2}} \tag{17a}$$

$$P_{doy} = -\frac{\pi \cdot D \cdot V_{ch0x}}{\sqrt{f^2 + \pi^2 \cdot D^2}} \tag{17b}$$

$$P_{doz} = \frac{f \cdot V_{ch0x}}{\sqrt{f^2 + \pi^2 \cdot D^2}} \tag{17c}$$

$$\boldsymbol{P}_{r0} = r_{ox} \cdot \boldsymbol{i} + r_{oy} \cdot \boldsymbol{j} + r_{oz} \cdot \boldsymbol{k} \tag{18}$$

$$r_{0x} = \sin\lambda_s \cdot a_{0y} - \cos\lambda_s \cdot \cos Kr \cdot a_{0z} \tag{19a}$$

$$r_{0y} = -\sin\lambda_s \cdot a_{0x} - \cos\lambda_s \cdot \sin Kr \cdot a_{0z} \tag{19b}$$

$$r_{0z} = \cos\lambda_s \cdot \sin Kr \cdot a_{0y} + \cos\lambda_s \cdot \cos Kr \cdot a_{0x} \tag{19c}$$

$$\boldsymbol{P}_{s0} = \boldsymbol{V}_{s0} \times \boldsymbol{b}_0 / |\boldsymbol{V}_{s0} \times \boldsymbol{b}_0| \tag{20}$$

$$\boldsymbol{n}_0 = \cos Kr \cdot \boldsymbol{i} + \sin Kr \cdot \boldsymbol{j} \tag{21}$$

where $\boldsymbol{P}_{b0}$ is the unit normal vector of the base plane of the tool P_r; $\boldsymbol{P}_{d0}$ is the unit normal vector of P_d, P_{dox},

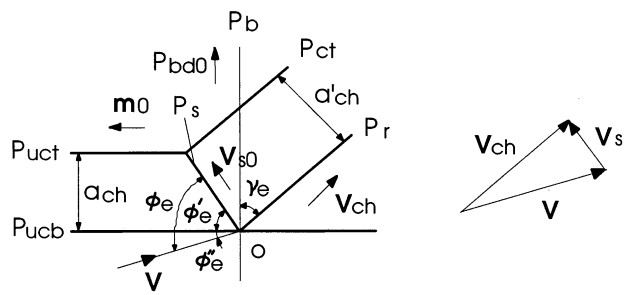

Fig. 3. Chip deformation plane P_d and the velocity triangle (P_b: base plane of tool; P_{ct}: top plane of the deformed chip; P_{uct}: top plane of the uncut layers of work material; P_{ucb}: bottom plane of the uncut layer of work material; P_r: the tool rake face; P_s: the shear plane).

P_{doy}, P_{doz} are respectively the x-, y-, and z-components of $\boldsymbol{P}_{d0}$; $\boldsymbol{P}_{r0}$ is the unit normal vector of P_r; r_{ox}, r_{oy}, r_{oz} are respectively the x-, y-, and z-components of $\boldsymbol{P}_{r0}$; $\boldsymbol{P}_{s0}$ is the unit normal vector of P_s; and $\boldsymbol{n}_0$ is the unit normal vector of the top plane of the uncut layer of work material P_{uct}.

The relating plane equations are as follows:

$$P_b: \quad z = 0 \tag{22}$$

$$P_d: \quad P_{dox} \cdot x + P_{doy} \cdot y + P_{doz} \cdot z = 0 \tag{23}$$

$$P_r: \quad r_{ox} \cdot x + r_{oy} \cdot y + r_{oz} \cdot z = 0 \tag{24}$$

$$P_{ct}: \quad r_{ox} \cdot x + r_{oy} \cdot y + r_{oz} \cdot z = a_{ch} \tag{25}$$

$$P_{uct}: \quad \cos Kr \cdot x + \sin Kr \cdot y = a_c \tag{26}$$

$$P_{ucb}: \quad \cos Kr \cdot x + \sin Kr \cdot y = 0 \tag{27}$$

where a_c is the undeformed chip thickness measured in the plane perpendicular to the bottom plane of the uncut layer of work material P_{ucb}; a_{ch} is the chip thickness measured in the plane perpendicular to P_r.

3.4. Effective rake angle of the tool and the effective shear angle

$$\boldsymbol{P}_{bd0} = \boldsymbol{P}_{d0} \times \boldsymbol{P}_{b0} / \left| \boldsymbol{P}_{d0} \times \boldsymbol{P}_{b0} \right| \tag{28}$$

$$\boldsymbol{m}_0 = \boldsymbol{P}_{d0} \times \boldsymbol{n}_0 / \left| \boldsymbol{P}_{d0} \times \boldsymbol{n}_0 \right| \tag{29}$$

$$\cos \gamma_e = \boldsymbol{V}_{ch0} \cdot \boldsymbol{P}_{bd0} \tag{30}$$

$$\cos \phi''_e = \boldsymbol{m}_0 \cdot \boldsymbol{V}_0 \tag{31}$$

$$a'_c = a_c \cdot \sqrt{\left(\frac{2P_{doy} \cdot \cos Kr - P_{dox} \cdot \sin Kr}{\sin Kr} \right)^2 + (P_{doy})^2 + (P_{doz})^2} \tag{32}$$

$$a'_{ch} = a_{ch} \tag{33}$$

$$tg\phi'_e = \frac{\cos \gamma_e}{a'_{ch}/a'_c - \sin \gamma_e} \tag{34}$$

$$\phi_e = \phi'_e + \phi''_e \tag{35}$$

where P_{bd0} is the unit vector parallel to the line of intersection between P_b and P_d; $\boldsymbol{m}_0$ is the unit vector parallel to the line of intersection between P_d and P_{uct}; γ_e is the effective rake angle of the tool; a'_c is the undeformed chip thickness measured in P_d; a'_{ch} is the chip thickness measured in P_d ($a'_{ch} = a_{ch}$); r is the cutting ratio; ϕ_e is the effective shear angle; and ϕ'_e and ϕ''_e are two angles used in the calculations.

3.5. Cutting force and cutting power

Supposing the shear stress in P_s is τ, the shear force $\boldsymbol{F}_\tau$ can be obtained from:

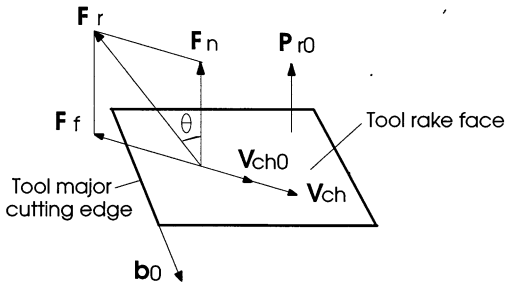

Fig. 4. Cutting forces on the tool rake face.

$$\boldsymbol{F}_\tau = (a_c \cdot a_w \cdot \tau) / (\boldsymbol{P}_{s0} \cdot \boldsymbol{k}) \cdot \boldsymbol{V}_{s0} \tag{36}$$

where a_w is the undeformed chip width.

The resultant cutting force on the tool rake face $\boldsymbol{F}_r$ can be decomposed into the component perpendicular to the tool rake face $\boldsymbol{F}_n$ and the component parallel to the tool rake face, i.e. the frictional force in the tool rake face $\boldsymbol{F}_f$, $\boldsymbol{F}_f$ is in the opposite direction to the chip flow velocity vector $\boldsymbol{V}_{ch}$. Fig. 4 shows the force on the tool rake face, where θ is the friction angle.

The unit vector parallel to the resultant cutting force $\boldsymbol{F}_{r0}$ is given by:

$$\boldsymbol{F}_{r0} = \cos \theta \cdot \boldsymbol{P}_{r0} - \sin \theta \cdot \boldsymbol{V}_{ch0} \tag{37}$$

Thus, the resultant cutting force $\boldsymbol{F}_r$ and the frictional force in the tool rake face $\boldsymbol{F}_f$ can be determined as:

$$\boldsymbol{F}_r = (\left| \boldsymbol{F}_\tau \right| / \left| \boldsymbol{F}_{r0} \cdot \boldsymbol{P}_{s0} \right|) \cdot \boldsymbol{F}_{r0} \tag{38}$$

$$\boldsymbol{F}_f = -\left| \boldsymbol{F}_r \right| \cdot \sin \theta \cdot \boldsymbol{V}_{ch0} \tag{39}$$

Due to nearly all of the cutting energy being consumed in two forms, i.e. the shear energy consumed in the shear plane and the friction energy consumed in the tool rake face [8], the cutting power A can be obtained from:

$$A = \left| \boldsymbol{F}_\tau \right| \cdot \boldsymbol{V}_s + \left| \boldsymbol{F}_f \right| \cdot \boldsymbol{V}_{ch} \tag{40}$$

The above equations, Eqs. (1)–(3), (3b), (3c)–(5), (5b), (5c)–(17), (17b), (17c)–(19), (19b) and (19c)–(40), are the theoretical calculations based on the improved model for oblique cutting. The input parameters for the model are: the normal rake angle of the tool γ_n; the tool cutting edge inclination angle λ_s; the tool major cutting edge angle Kr; the cutting speed V_c; the tool feed speed V_f; the undeformed chip width a_w; the shear stress τ; the friction angle θ; the chip flow angle η; and the cutting ratio r. The important output parameters from the model include: the effective rake angle of the tool γ_e; the effective shear angle ϕ_e; and the cutting power A; etc.

As a practical example, the above-established model is used in the following chip-control research to investigate the relationships between the said input parameters and the relating output parameters.

4. Application of the model to the chip-control research

4.1. Brief introduction of a theory on the minimum energy consumption

A theory on the minimum energy consumption is presented in the literature [14,15]. The theory is used to investigate the chip flow coordination and chip flow interference during machining processes. It studies the physical substance of chip flow, i.e. why the chip flows away from the tool rake face in this direction, but not in that direction, during machining processes.

As is known, a whole cutting edge can be divided into a series of infinitesimal cutting edges called elemental cutting edges. Every elemental cutting edge has a straight line cutting edge and cuts the work material in the oblique form. For a definite elemental cutting edge, there must exist a definite chip flow vector, which consists of a definite chip flow direction and a definite chip flow speed. This definite chip flow vector is known as the natural chip flow vector. In terms of the theory on the minimum energy consumption, the physical substance of the chip flow vector is to make the total consumption of cutting power be the minimum. When the natural chip flow vectors produced by the different elemental cutting edges interfere with each other, the total chip flow vector for the whole cutting edge can be determined in the light of the rule that makes the total consumption of cutting power be the minimum: this is not an artificial optimum, but a natural choice.

4.2. Calculation of the chip flow vector

Based on the established model, with the values of γ_n, λ_s, Kr, V_c, V_f, a_w, τ and θ being given, the cutting power A can be regarded as the function of the chip flow angle η and the cutting ratio r, i.e.:

$$A = f(r, \eta) \tag{41}$$

In the oblique cutting, with the above relating parameters being given, according to the theory on the minimum energy consumption, there must exist definite values of η and r which makes the consumption of cutting power be the minimum.

Therefore, the established model is input into a computer to optimise the cutting power A and to find two definite values of η and r which make the consumption of cutting power be the minimum. The chip flow speed can be obtained from Eq. (13) after the value of r has been determined.

4.3. Oblique cutting experiment

The experimental conditions are as follows: Machine tool, VDF 18 RO lathe; Workpiece, AISI 1088 steel tube with a diameter 42.6 mm; Tool holder, T-MAX PTTNR 2020K 16; Tool insert, TNMA 160404 (HK 15); Tool geometry, $\gamma_n = -6°$, $\lambda_s = -6°$, $Kr = 45° \sim 90°$; Cutting form, oblique cutting with no cutting fluid; and Cutting parameters, $V_c = 95$ m min^{-1}, $V_f = 71 \sim 355$ mm min^{-1}, $a_p = 3.25$ mm.

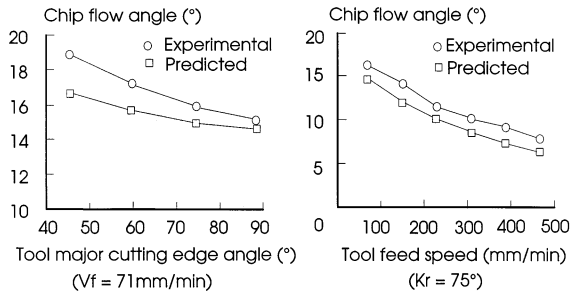

Fig. 5. Influence of the tool major cutting edge angle Kr and the tool feed speed V_f on the chip flow angle η.

The chip flow angle is measured with a measuring microscope by observing the frictional trace caused by the flow of the chip on the tool rake face.

Fig. 5 shows the comparison of the chip flow angle between the theoretical predictions and the experimental results under the said given experimental conditions; whilst Fig. 6 shows the variation of the chip flow speed calculated from Eq. (13).

From Fig. 5, it can be seen that the theoretically-predicted data agrees reasonably well with the experimental results under the given experimental conditions.

5. Conclusions

Based on the above investigation, the following conclusions can be drawn:

(1) An improved model for oblique cutting has been developed in this present work in which the influences of the tool major cutting edge angle and the tool feed velocity on machining processes are taken account of.

(2) The new cutting model can be used to determine precisely some important parameters involved in machining processes, e.g. the effective rake angle of the tool, the effective shear angle and the consumption of cutting power, etc.

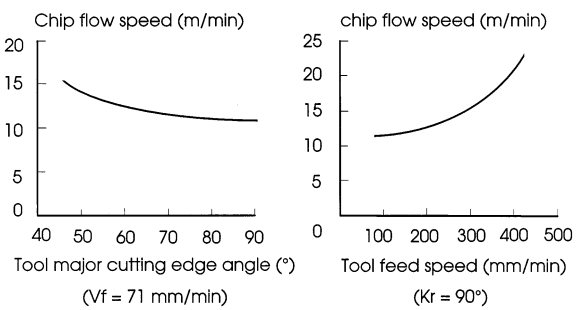

Fig. 6. Variation of the chip flow speed V_{ch}.

(3) As a practical example, the model, combined with the theory on minimum energy consumption, is used to carry out chip-control research. The chip flow direction and the chip flow speed are determined based on the model and the theory on minimum energy consumption.

(4) The theoretically-predicted data agrees reasonably well with the experimental results under the given experimental conditions.

6. Nomenclature

A	cutting power
a_c	undeformed chip thickness measured in the plane perpendicular to P_{ucb}
a'_c	undeformed chip thickness measured in P_d
a_{ch}	chip thickness measured in the plane perpendicular to P_r
a'_{ch}	chip thickness measured in P_d
$\boldsymbol{a}_0$	unit vector in the tool rake face perpendicular to the tool major cutting edge
a_{0x}, a_{0y}, a_{0z}	x-, y-, and z-components of $\boldsymbol{a}_0$, respectively
a_p	depth of cut
a_w	undeformed chip width
$\boldsymbol{b}_0$	unit vector in the tool rake face parallel to the tool major cutting edge
D	diameter of the workpiece
$\boldsymbol{F}_f$	frictional force in P_r
$\boldsymbol{F}_r$	resultant cutting force on P_r
$\boldsymbol{F}_{r0}$	unit vector parallel to $\boldsymbol{F}_r$
$\boldsymbol{F}_n$	cutting force component perpendicular to P_r
$\boldsymbol{F}_\tau$	shear force on P_s
f	feed of the tool per revolution
$\boldsymbol{i}$, $\boldsymbol{j}$, $\boldsymbol{k}$	unit vector along the x-, y-, and z-axes, respectively
Kr	tool major cutting edge angle
$\boldsymbol{m}_0$	unit vector parallel to the line of intersection between P_d and P_{uct}
n	speed of the spindle of machine tool
$\boldsymbol{n}_0$	unit normal vector of P_{uct}
$\boldsymbol{P}_b$	base plane of tool
$\boldsymbol{P}_{b0}$	unit normal vector of P_b
$\boldsymbol{P}_{bd0}$	unit vector parallel to the line of intersection between P_b and P_d
P_{ct}	top plane of the deformed chip
P_d	chip deformation plane
$\boldsymbol{P}_{d0}$	unit normal vector of P_d
P_{dox}, P_{doy}, P_{doz}	x-, y-, and z-components of $\boldsymbol{P}_{d0}$, respectively
P_r	tool rate face
$\boldsymbol{P}_{r0}$	unit normal vector of P_r
P_s	shear plane
$\boldsymbol{P}_{s0}$	unit normal vector of P_s
P_{ucb}	bottom plane of the uncut layer of work material
P_{uct}	top plane of the uncut layer of work material
r	cutting ratio
r_{ox}, r_{oy}, r_{oz}	x-, y-, and z-components of $\boldsymbol{P}_{r0}$, respectively
$\boldsymbol{V}$	resultant cutting velocity vector
$\boldsymbol{V}_c$	cutting velocity vector
$\boldsymbol{V}_{ch}$	chip flow velocity vector
$\boldsymbol{V}_{ch0}$	unit vector parallel to $\boldsymbol{V}_{ch}$
V_{ch0x}, V_{ch0y}, V_{choz}	x-, y-, and z-components of $\boldsymbol{V}_{ch0}$, respectively
$\boldsymbol{V}_f$	tool feed velocity vector
$\boldsymbol{V}_0$	unit vector parallel to $\boldsymbol{V}$
$\boldsymbol{V}_s$	shear velocity vector
$\boldsymbol{V}_{s0}$	unit vector parallel to $\boldsymbol{V}_s$

Greek letters

γ_n	normal rake angle of the tool
γ_e	effective rake angle of the tool
ϕ_e	effective shear angle
ϕ'_e, ϕ''_e	angles used in the calculations
λ_s	tool cutting edge inclination angle
τ	shear stress in P_s
θ	friction angle on P_r
η	chip flow angle

References

[1] B.L. Juneja, G.S. Sekhon, Fundamentals of Metal Cutting and Machine Tools, Wiley Eastern Ltd., New Delhi, 1987.

[2] T.C. Hsu, C.Y. Choi, Measurement and representation of cutting force due to oblique machining, Int. J. Mach. Tool Des. Res. 10 (1970) 49–55.

[3] W.K. Luk, Mechanics of turning operations, Int. J. Mach. Tool Des. Res. 10 (1970) 351–356.

[4] W.A. Morcos, A solution to the free oblique continuous cutting problem in condition of light friction at tool–chip interface, Trans. ASME 14 (1972) 1124–1131.

[5] R.H. Brown, E.J.A. Amerego, Oblique machining with a single cutting edge, Int. J. Mach. Tool Des. Res. 4 (1964) 9–16.

[6] P.L.B. Oxley, An analysis for orthogonal cutting with restricted tool-chip contact, Int. J. Mech. Sci. 4 (1962) 129–135.

[7] K. Iwata, K. Osakada, Processing modelling of orthogonal cutting by rigid finite element method, Trans. ASME 106 (1986) 132–138.

[8] M.C. Shaw, Metal Cutting Principles, Clarendon, Oxford, 1984.

[9] N.N. Zorev, Metal Cutting Mechanics, Pergamon Press, Oxford, 1966.

[10] E.M. Trent, Metal Cutting, Butterworths, London, 1977.

[11] E. Usui, Modern Theory of Metal Cutting, Kyoritsu Shuppan, Tokyo, 1990.

[12] G. Boothroyd, Fundamentals of Metal Machining and Machine Tools, McGraw-Hill, London, 1975.

[13] V. Arshinor, G. Alekseev, Metal Cutting Theory and Cutting Tool Design, 1970 Mir Publications, Moscow, 1970.
[14] N. Fang, M. Wang, On the consumption of cutting power influenced by chip flow under non-free cutting conditions, Chinese J. Mech. Eng. 1 (1997) 37–43 (English Edition).
[15] N. Fang, The study of new-type chip breaking groove geometry of indexable cemented carbide inserts and related CAD technology, PhD Thesis, Huazhong University of Science and Technology, Wuhan, P.R. China, 1994.
[16] N. Fang, Y.J. Chen, Chip disposal during maching of 1Cr18Ni9Ti with indexable inserts, J. Huazhong Univ. Sci. Tech. 22 (2) (1994) 11–16.
[17] N. Fang, The study and design of chip breaking groove geometry of indexable inserts, Cemented Carbide 10 (1) (1993) 21–25.
[18] K. Nakayama, Chip control in metal cutting, Bull. JSPE 18 (2) (1984) 97–103.
[19] I.S. Jwahiar, C.A. Luttervelt, Recent developments in chip control research and applications, Annals. CIRP 42 (2) (1993) 659–685.